

Mapping of RNA modifications by direct Nanopore sequencing and JACUSA2

Christoph Dieterich^{*1,2,3}, Amina Lemsara^{1,2}, and Isabel Naarmann-de Vries^{1,2,3}

¹Klaus Tschira Institute for Integrative Computational Cardiology, University Heidelberg, 69120 Heidelberg, Germany

²Department of Internal Medicine III (Cardiology, Angiology, and Pneumology), University Hospital Heidelberg, 69120 Heidelberg, Germany

³German Centre for Cardiovascular Research (DZHK)-Partner Site Heidelberg/Mannheim, 69120 Heidelberg, Germany

Abstract

to be written

Keywords: Bayesian, 10X Genomics, Cell barcode assignment, Nonsense-mediated mRNA decay (NMD)

INTRODUCTION

Chemical modifications on DNA and histones, also known as epigenetics marks, strongly impact gene expression during cell differentiation and in several other biological programs. In the 1970s, it was recognized that RNA is also subjected to extensive covalent modification, and studies in the late 1980s revealed the widespread deamination of bases (termed RNA editing), which can lead to recoding if it occurs within coding sequences. Impressive development in the RNA modification field occurred during the past eight years, with the discovery of an extensive layer of base modifications in mRNAs. These can influence gene expression and have been already shown to be involved in primary cellular programs such as stem cell differentiation, response to stress, and the circadian clock. The study of RNA modifications and their effects is now referred to as epitranscriptomics, and it reveals striking similarities to what is known for epigenomics. To date thirteen distinct modifications have been identified on mRNA transcripts [Anreiter et al., 2021]. These modifications are catalyzed by a variety of dedicated enzymes and can be divided into two classes: modifications of cap-adjacent nucleotides and internal modifications.

*christoph.dieterich@uni-heidelberg.de

32 In contrast to the m7G cap, the impact of internal modifications on gene
 33 regulation has been less studied apart from RNA editing, which is mediated
 34 by RNA deaminases (e.g. the ADAR family). The most widespread in-
 35 ternal mRNA modification is N6-methyladenosine (m6A). By modulating
 36 the processing of mRNA, m6A can regulate a wide range of physiological
 37 processes and its alteration has been linked to several diseases Roignant
 38 and Soller [2017], Zaccara et al. [2019], Shi et al. [2019]. The modification is
 39 catalyzed co-transcriptionally by a Mega-Dalton methyltransferase complex,
 40 which includes the heterodimer METTL3-METTL14 and other associated
 41 subunits Garcias Morales and Reyes [2021]. This modification is reversible
 42 since two proteins of the AlkB-family demethylases can remove m6A from
 43 mRNA transcripts [Jia et al., 2011, Zheng et al., 2013]. In mammals, m6A
 44 preferentially localizes within long internal exons and at the beginning of
 45 terminal exons at so-called DRACH motif (D = A/G/U, R = A/G, H =
 46 A/C/U) sites [Dominissini et al., 2012, Meyer et al., 2012, Ke et al., 2015].
 47 Once deposited, m6A is recognized by several reader proteins that can af-
 48 fect the fate of mRNA transcripts in nearly every step of the mRNA life
 49 cycle, which includes alternative splicing [Adhikari et al., 2016, Roundtree
 50 et al., 2017]. The best-described readers are the YTH domain family of
 51 proteins that decode the signal and mediate m6A functions. By affecting
 52 RNA structure, m6A can also indirectly influence the association of addi-
 53 tional RNA-binding proteins (RBPs) and the assembly of larger messenger
 54 ribonucleoprotein particles (mRNPs).

55 Several approaches have been presented to map RNA modifications on
 56 RNA. Herein, we focus on mRNA modification site detection in general and
 57 on m6A in particular where antibody-based protocols (miCLIP), methylation-
 58 sensitive restriction enzyme assays (MazF) or transgenic approaches (TRIBE,
 59 DART) have been presented. All of the aforementioned approaches rely on
 60 high-throughput sequencing on the Illumina platform. This typically in-
 61 volves cDNA synthesis by reverse transcription and PCR-based library am-
 62 plification. One recent addition to the tool is direct RNA single molecule
 63 sequencing on the Oxford Nanopore Technology platform. While or software
 64 workflow is able to deal with Illumina and Nanopore-based approaches, the
 65 latter is the principal topic of our methods article.

66 MATERIALS

67 ONT direct RNA sequencing

- 68 1. 500 ng polyA⁺ RNA isolated from total RNA e.g. with Oligotex
 69 mRNA kit (Qiagen) or Dynabeads oligo dT₂₅ beads (Thermo Fisher
 70 Scientific) or *in vitro* transcriptome sample. Store RNA at -80 °C and
 71 the mRNA purification kit as recommended by the manufacturer.

- 72 2. Nuclease-free water. Store at room temperature.
- 73 3. Direct RNA-sequencing kit (SQK-RNA002, Oxford Nanopore Tech-
74 nologies). Store at -20 °C.
- 75 4. NEBNext Quick Ligation Reaction Buffer (New England Biolabs).
76 Store at -20 °C.
- 77 5. T4 DNA Ligase (New England Biolabs). Store at -20 °C.
- 78 6. dNTP Mix (10 mM each). Store at -20 °C.
- 79 7. SuperScript IV Reverse Transcriptase (Thermo Fisher Scientific). Store
80 at -20 °C.
- 81 8. Agencourt RNAClean XP beads (Beckman Coulter). Store at 4 °C.
- 82 9. 70 % ethanol, freshly prepared.
- 83 10. Qubit dsDNA HS assay kit and Qubit Fluorometer (Thermo Fisher
84 Scientific).
- 85 11. Flow cell priming kit (EXP-FLP002, Oxford Nanopore Technologies).
86 Store at -20 °C.
- 87 12. Thermocycler.
- 88 13. Gentle rotator mixer.
- 89 14. Magnetic stand for 1.5 ml tubes.
- 90 15. 1.5 ml DNA LoBind tubes (Eppendorf), 0.2 ml PCR tubes.
- 91 16. MinION or GridION sequencing device and MinION R9.4.1 Flow cells
92 (FLO-MIN106D, Oxford Nanopore Technologies). Store Flow cells at
93 4 °C.

94 **Preparation of an *in vitro* transcriptome sample**

- 95 1. 100 ng polyA⁺ RNA isolated from total RNA e.g. with Oligotex
96 mRNA kit (Qiagen) or Dynabeads oligo dT₂₅ beads (Thermo Fisher
97 Scientific). Store RNA at -80 °C and the mRNA purification kit as
98 recommended by the manufacturer
- 99 2. 10 μM oligo(dT)-VN RT primer. TTTTTTTTTTTTTTTTTTTTTTTTTTTTTTTVN.
100 Store at -20 °C.
- 101 3. 20 μM template switching oligo (TSO). ACTCTAATACGACTCAC-
102 TATAGGGAGAGGGCrGrG+G. Store at -20 °C.

- 103 4. 10 μ M T7 extension primer. GCTCTAATACGACTCACTATAGG.
104 Store at -20 °C.
- 105 5. Nuclease-free water. Store at room temperature.
- 106 6. dNTP Mix (10 mM each). Store at -20 °C.
- 107 7. Template Switching RT Enzyme Mix (New England Biolabs). Store
108 at -20 °C.
- 109 8. Q5 Hot Start High-Fidelity 2X Master Mix (New England Biolabs).
110 Store at -20 °C.
- 111 9. RNase H (5,000 U/ml) (New England Biolabs). Store at -20 °C.
- 112 10. NucleoSpin Gel and PCR Clean-up, Mini kit for gel extraction and
113 PCR clean up (Macherey-Nagel) or equivalent. Store at room temper-
114 ature.
- 115 11. MEGAscript T7 transcription kit (Thermo Fisher Scientific). Store at
116 -20 °C.
- 117 12. RNA Clean & Concentrator-25 kit (Zymo Research). Store at room
118 temperature.
- 119 13. Thermocycler.
- 120 14. Table top centrifuge for 1.5 ml tubes.
- 121 15. Nanodrop spectrophotometer or equivalent.
- 122 16. 0.2 ml PCR tubes, 1.5 ml DNA LoBind tubes (Eppendorf).

123 **Hardware requirements**

124 All analyses have been performed/tested on two alternative hardware sys-
125 tems: a standard Linux desktop computer or an Apple iMac (Retina 5K,
126 ultimo 2014). The workflow requires a multi-core processor system with
127 minimal main memory of 16GB RAM and several GBs of free disk space
128 (depending on data set size).

129 **Software dependencies and installation**

130 Our analysis workflow has few requirements, which are detailed in Table 2.
131 Specifically, to execute our workflow, the following prerequisites are neces-
132 sary: a BASH shell, a JAVA runtime environment, a working PERL and
133 R installation. Additional i.e. non-standard software to process and map
134 Nanopore reads (bedtools, samtools and Minimap2) are obligatory, while

135 the installation of a Nanopore read simulator (NanoSim) is optional and de-
136 pends on your use case. Table ?? lists some additional R packages, which are
137 required to run the R code. Detailed instructions on how to setup are found
138 under https://github.com/dieterich-lab/MiMB_JACUSA2_chapter

139 METHODS

140 Overview Figure 1

141 Nanopore direct RNA sequencing

- 142 1. Adjust 500 ng polyA⁺ RNA to a total volume of 9 μ l with nuclease-
143 free water. Complete RT adapter ligation reaction (in 0.2 ml PCR
144 tube) with 3 μ l NEBNext Quick Ligation Reaction Buffer, 0.5 μ l
145 RNA CS (RCS, from SQK-RNA002), 1 μ l RT-Adapter (RTA, from
146 SQK-RNA002) and 1.5 μ l T4 DNA Ligase. Incubate 10 min at room
147 temperature.
- 148 2. Prepare reverse transcription master mix on ice during ligation: 9 μ l
149 nuclease-free water, 2 μ l 10 mM dNTPs, 8 μ l 5x SuperScript IV first
150 strand buffer, 4 μ l 0.1 mM DTT.
- 151 3. Add the reverse transcription master mix to the ligation reaction and
152 mix by pipetting. Add 2 μ l SuperScript IV reverse transcriptase and
153 mix by pipetting. Incubate in a thermocycler with the following pro-
154 tocol: 50 min at 50 °C, 10 min at 70 °C, cool down to 4 °C.
- 155 4. Let the Agencourt RNAClean XP beads come to room temperature
156 during reverse transcription. Carefully resuspend beads before use.
157 Transfer reaction to a 1.5 ml DNA LoBind tube and mix with 72 μ l
158 Agencourt RNAClean XP beads. Incubate 5 min at room temperature
159 on a gentle rotator mixer.
- 160 5. Collect beads on a magnetic stand and remove supernatant. Wash
161 pelleted beads two times (30 sec) with 200 μ l freshly prepared 70 %
162 ethanol. Remove supernatant. Spin sample down and place on magnet
163 again. Remove any residual ethanol.
- 164 6. Resuspend beads in 20 μ l nuclease-free water by gentle flicking and
165 incubate 5 min at room temperature on a gentle rotator mixer. Collect
166 beads on a magnetic stand and transfer 20 μ l eluate in a fresh 1.5 ml
167 DNA LoBind tube.
- 168 7. For ligation of the RMX adapter, add the following to 20 μ l eluate: 8
169 μ l NEBNext Quick Ligation Reaction Buffer, 6 μ l RMX (from SQK-
170 RNA002), 3 μ l nuclease-free water, 3 μ l T4 DNA Ligase. Mix by
171 pipetting and incubate 10 min at room temperature.

- 172 8. Add 40 μ l carefully resuspended Agencourt RNAClean XP beads to
173 the reaction and mix by pipetting. Incubate 5 min at room tempera-
174 ture on a gentle rotator mixer.
- 175 9. Collect beads on a magnetic stand and remove supernatant. Wash
176 pelleted beads two times with 150 μ l wash buffer (WSB, from SQK-
177 RNA002). Resuspend beads by flicking, spin down and return to mag-
178 netic stand. Remove supernatant from pelleted beads.
- 179 10. Resuspend beads in 21 μ l elution buffer (EB, from SQK-RNA002) by
180 gentle flicking and incubate 5 min at room temperature on a gentle
181 rotator mixer. Pellet beads on a magnetic stand and transfer 21 μ l
182 eluate in a fresh 1.5 ml DNA LoBind tube.
- 183 11. Quantify 1 μ l of the library on a Qubit fluorometer with the Qubit
184 dsDNA HS kit according to the manufacturerers protocol. Concentra-
185 tion should be usually in the range of 5 - 10 ng/ μ l.
- 186 12. Insert MinION R9.4.1 Flow cell in the MinION or GridION sequenc-
187 ing device and perform Flow cell check in the MinKNOW software.
188 For successful sequencing of mammalian polyA⁺ RNA at least 1,000
189 available pores are recommended.
- 190 13. Prepare Priming Mix by adding 30 μ l flush tether (FLT, from EXP-
191 FLP002) to a vial of flush buffer (FB, from EXP-FLP002) and mix by
192 pipetting. Open priming port. Remove air bubble from priming port
193 by inserting the tip of a P1000 pipette into the priming port and slowly
194 dialing up, until a small volume of storage buffer enters the pipette
195 tip. Load 800 μ l Priming Mix via the priming port and carefully avoid
196 introduction of air bubbles. Close the priming port and wait for 5 min.
- 197 14. Mix 20 μ l library with 17.5 μ l nuclease-free water and 37.5 μ l RNA run-
198 ning buffer (RRB, from SQK-RNA002) and mix by pipetting. Open
199 the priming port and the sample port. Load 200 μ l Priming Mix via
200 the priming port. Mix library by pipetting just before loading and
201 load dropwise via the sample port. Carefully avoid introduction of air
202 bubbles. Close the sample port and the priming port.
- 203 15. Start sequencing for 48 to 72 h in the MinKNOW software. Choose
204 direct RNA-sequencing kit and high-accuracy basecalling as paramet-
205 ers. We recommend to adjust the output filter to a minimum Q score
206 of 7 (instead of 9).

207 Preparation of an *in vitro* transcriptome sample

208 The *in vitro* transcriptome sample is prepared based on a protocol published
209 by Zhang *et al.* Zhang et al. [2021] with some modifications.

- 210 1. Adjust 100 ng polyA⁺ RNA to a total volume of 6 μ l with nuclease-
211 free water. Add 1 μ l each of 10 μ M oligo(dT)-VN RT primer and 10
212 mM dNTPs. Mix by pipetting and incubate in a thermocycler: 5 min
213 at 75 °C, 2 min at 42 °C, cool to 4 °C.
- 214 2. Assemble 2.5 μ l 4x template switching RT buffer, 0.5 μ l 20 μ M TSO,
215 1 μ l 10x template switching RT enzyme mix and mix by pipetting.
216 Combine with 6 μ l RNA and incubate in a thermocycler: 90 min at
217 42 °C, 10 min at 68 °C, cool to 4 °C.
- 218 3. For Second strand synthesis add to First strand synthesis reaction: 50
219 μ l Q5 Hot Start High-Fidelity 2X Master Mix, 5 μ l RNase H, 2 μ l 10
220 μ M T7 extension primer, 33 μ l nuclease-free water. Mix by pipetting
221 and incubate in a thermocycler: 15 min at 37 °C, 1 min at 95 °C, 10
222 min at 65 °C, cool to 4 °C.
- 223 4. Purify double stranded cDNA with NucleoSpin Gel and PCR Clean-up
224 kit according to the manufacturerers protocol and elute in 20 μ l elution
225 buffer. Determine concentration on a Nanodrop spectrophotometer.
226 cDNA may be stored at -20 °C.
- 227 5. Combine 8 μ l cDNA for *in vitro* transcription with 2 μ l each of ATP,
228 GTP, CTP, UTP, 10x reaction buffer and enzyme mix from the MEGAscript
229 T7 transcription kit. Incubate 3 h at 37 °C.
- 230 6. Digest template DNA by addition of 1 μ l Turbo DNase. Mix by pipet-
231 ting and incubate 15 min at 37 °C.
- 232 7. Adjust reaction volume to 100 μ l with nuclease-free water and clean up
233 with RNA Clean & Concentrator-25 kit according to the manufactur-
234 ers protocol, using two volumes of adjusted RNA binding buffer (1:1
235 RNA binding buffer : ethanol). Elute RNA in 25 μ l nuclease-free wa-
236 ter. Determine RNA concentration on a Nanodrop spectrophotometer.
237 Store at -80 °C.

238 Nanopore read processing

- 239 1. Base call the ionic current signal stored in FAST5 file using Guppy.
240 For the IVT readout, we adopted real-time base calling with the
241 MinKNOW-embedded Guppy basecaller. Otherwise, Guppy base-
242 caller software can be used; in this case, the basecaller requires the
243 path to FAST5 files, the output folder, and the config file or the flow-
244 cell/kit combination. The output is FASTQ files that can be com-
245 pressed using the option "--compress_fastq".

```

246 $ guppy_basecaller --compress_fastq -i path_to_fast5 -s path_to_output
247 -c config_file.cfg --cpu_threads_per_caller 14 --num_callers
248 1
249 Set the number of threads "cpu_threads_per_caller" and the number
250 of parallel basecallers "num_caller" according to your resources. Ad-
251 ditional details can be found in Gup [2019].

```

2. Align reads to the transcriptome using Minimap2 software. The output is a SAM file that has to be converted to a compressed form as BAM file using SAMtools command. The alignment requires the reference sequence. Here, we used GRCh38 Ensembl annotation and FASTA file release version 96. **To reduce the indexing time of the human genome, save the index with the option "-d" before the mapping and use the index instead of the reference file in the minimap2 command line.**

```

260 $ minimap2 -d reference.mmi reference.fa

```

To allow spliced alignments, use the setting "-ax splice -junc-bed annotation.bed -junc-bonus" where "-junc-bonus" allows to tune the bonus score and the BED file "-junc-bed annotation.bed" provides the splice junctions. The BED file can be generated using the following command:

```

266 $paftools.js gff2bed annotation.gtf > annotation.bed

```

Use "-ub" to allow alignment to both strands or '-uf' to force the alignment to only forward strand. For Direct RNA Sequencing, it is recommended to set a small k-mer size "-k [=14]" to enhance sensitivity. We recommend outputting primary alignments "-secondary=no". Use the parameter '-MD' to add the reference sequence information to the alignment; this is recommended for the downstream analysis. Customize the number of threads "-t" according to your resources. Check Minimap2 manual for more details [Min].

```

275 $ minimap2 -t 5 --MD -ax splice --junc-bonus 1 -k14 --secondary=no
276 --junc-bed final_annotation_96.bed -ub reference.mmi Reads.fastq.gz
277 |samtools view -bS > mapping.bam

```

3. Map RNA modifications using JACUSA2 pipeline. JACUSA2 [Piechotta et al., 2021] rapidly detects RNA modifications based on a comparative strategy where the mapping features (mismatch, insertion and deletion) of a sample of interest is compared to a reference sequence (call-1) or against a sample without RNA modifications, e.g. a knock-out of an RNA modifying enzyme or an IVT (call-2). Moreover, it allows the integration of information from replicate experiments. **The output**

of JACUSA2 variant calling is a set of scores reflecting the read signatures involving mismatch, insertion and deletion. The analysis of read signature can be used for RNA modification detection. We integrate JACUSA2, in particular call-2 method, with the downstream analysis in one pipeline using the Python-based workflow management system Snakemake [Köster and Rahmann, 2012]. The Snakemake pipeline involves rules for the variant calling using JACUSA2 call-2, detection of RNA modification patterns, prediction of new modified sites and other intermediate rules as shown in figures 4. The input of the pipeline are BAM files from paired conditions with different replicates. BAM files need to be sorted and may be subjected to many filters before being used by JACUSA2 call2 rule. Here, we suggest to filter out secondary and poor alignments. The output of JACUSA2 call2 is preprocessed (get_features) and subjected to a learning process to extract and visualize modification patterns (resp. get_pattern, visualize_pattern) and make predictions (predict_modification). "split_train_test" rule allows splitting input data into a training set and a test set. To use our snakemake-based JACUSA2 pipeline a set of parameters should be defined in the "config.yaml" file; mainly: the label of the analysis 'label', the input bam files under 'data', the reference sequence 'reference', a file containing size of chromosomes 'chr_size', JACUSA2 jar file 'jar', plus the path to inputs and outputs under 'path_inp' and 'path_out' fields respectively. Further details on how to use JACUSA2 pipeline is presented within the use cases in the next section. The pipeline could be executed on a high-performance-computing cluster (HPC) using the following command by specifying the number of cores to be used "--cores [=all]" and the rule name:

```
$ srun snakemake --cores all rule_name
```

Check Snakemake documentation for more details [sna].

Use Case 1: Comparison of wild-type and knock-out samples

The conventional way to detect RNA modifications using direct RNA sequencing is to compare a modified sample to an unmodified control sample. To assess the ability of JACUSA2 in this case, we used a published dataset of HEK293 cell lines to detect m6A modification [Pratanwanich et al., 2021]. The benchmark is composed of two sample sets from two conditions: wild-type cells (modified RNAs) and Mettl3 knockout cells (unmodified RNAs) with two replicates (2 and 3). The FASTQ files are mapped using Minimapp2 as described in the previous section. The following analysis is validated against reported m6A sites in the three miCLIP-based studies Boulias et al. [2019], Koh et al. [2019], Körtel et al. [2021] (figure 5).

325 Given the preprocessed mapped reads as inputs (BAM files): 'HEK293T-
 326 WT-rep2.bam' and 'HEK293T-WT-rep3.bam' representing the wildtype repli-
 327 cates and 'HEK293T-KO-rep2.bam' and 'HEK293T-KO-rep3.bam' as the
 328 control replicates,

329 1. Identify read error profile: use "jacusa2_call2" rule to run JACUSA2
 330 in pairwise conditions mode (call-2). The method requires BAM files
 331 of the paired conditions and the corresponding library information "-
 332 P1" and "-P2". In addition to the mismatch score, add "-D" and "-I"
 333 to output the deletion and insertion scores. JACUSA2 allows filtering
 334 reads according to many parameters. Here, we consider all sites with
 335 base calling quality "-q [> 1]", mapping quality "-m [> 1]" and read
 336 coverage "-c [> 4]". Plus, it provides a filter feature to improve sensi-
 337 tivity. Here, we consider filtering sites within homopolymer regions "-a
 338 [=Y]". The output (named here, "Cond1vsCond2Call2.out") consists
 339 of a read error profile where the format is a combination of BED6 with
 340 JACUSA2 call-2 specific columns and common info columns: info, fil-
 341 ter, and ref. Check JACUSA2 manual for more details on JACUSA2
 342 filter and output options [JAC, 2021]. The number of threads can
 343 be customized via the parameter "-p". All parameters related to JA-
 344 CUSA2 method can be added under the field "jacusa_params" in the
 345 config file by setting the name of the parameter followed by the cor-
 346 responding value [key: value]. Be aware to set all parameters before
 347 running the pipeline.

348 \$ srun snakemake --cores all jacusa2_call2 \$

349 2. Preprocess JACUSA2 output: from JACUSA2 call-2 output, we select
 350 all sites within 5-mer of a central nucleotide 'A' flanked by 2 random
 351 nucleotides (NNANN) and we filter out sites of the homo-polymer re-
 352 gions (JACUSA filter: Y). Then, we rebuild the tabular features such
 353 that the observations are only sites with a reference base 'A'. Each
 354 site is characterized by 15 features corresponding to the mismatch,
 355 insertion and deletion scores for the observed site and its two flank-
 356 ing positions from both sides. The rule "get_features" performs the
 357 preprocessing step. Use the parameter 'region' with a file containing
 358 target 5-mers to limit the analysis to specific sites. The output is an
 359 R object "features/features.rds", representing the matrix of Sites×15
 360 features.

361 \$ srun snakemake --cores all get_features

362 3. Extract m6A modification pattern: given the matrix of Sites×Features,
 363 the next step is to learn a model representing the m6A modification
 364 pattern. To this end, the conventional non-negative matrix factoriza-
 365 tion (NMF) analysis is suggested [Lee and Seung, 1999]. Briefly, NMF

factorizes a non-negative data matrix X (here: n sites and m features) into two non-negative matrices as $X \approx WH$, such that W is an $n \times k$ matrix containing basis vectors and H is an $k \times m$ matrix containing coefficient vectors. The coefficient vectors and their combination can be viewed as a pattern for m6A modification. The rank of factorization k is a critical parameter that affects the performance substantially. We suggest to select the rank k according to the method of Frigyesi and Höglund [2008] by looking at silhouette [Rousseeuw, 1987] and cophenetic correlation [Brunet et al., 2004] indices. Accordingly, the performance indices are computed for different choices of rank ($k < n, m$) and compared to the performance of a random permutation of the original data. Subsequently, the chosen rank corresponds to the value with the largest difference between slopes of the original and the randomized data. Here, the unsupervised pattern training is based on the consensus set of 2,401 m6A sites reported in the three miCLIP-based studies mentioned earlier. Based on the silhouette and cophenetic correlation indices, we could identify an optimal factorization rank of 6 (figure 6A). We then analyzed the identified patterns. According to the membership indicator of each site in matrix W , more than 80% of m6A modification sites can be represented by five patterns (Patterns 1,2,3,4,6) (figure 6B). Interestingly, the linear combination of these five patterns in figure (6C) highlights the importance of position 3 and eventually the implication of all scores.

Using the JACUSA2 pipeline, run rule "get_pattern" to generate patterns and provide the set of modified sites as a ground truth under the field "modified_sites" in the config file. Here, the "miCLIP_union.bed" file contains the m6A sites from the three miCLIP-based studies. A miCLIP annotation, reflecting studies (hence, the consensus) wherein the modification is reported, is added to each site. A subset of modified sites could be used to generate patterns. Accordingly, the "internal_pattern" field should refer to the annotation of selected sites from the "modified_sites" file. Plus, multiple combinations of patterns can be defined and appended to the field "combined_pattern" as new patterns. The corresponding outputs are under "patterns" folder.

```
$ srun snakemake --cores all get_pattern
```

The produced patterns and their combinations can be visualized using "visualize_pattern" rule. The corresponding outputs are under "pattern/viz" folder.

```
$ srun snakemake --cores all visualize_pattern
```

4. Predict m6A modifications: the additive linear combination of the coefficient vectors (patterns) with the 15 features can be used to predict

407 m6A modification. We examine the ability of prediction on a sub-
 408 set of data of more than 1,98 million sites with 22,248 miCLIP m6A
 409 sites. We opt for the linear combination of the five important patterns
 410 described in step 3. The empirical Cumulative Distribution Function
 411 (eCDF) of the inferred scores shows clearly a significant difference be-
 412 tween the different miCLIP m6A categories (miCLIP annotation) and
 413 the unmodified sites (figure 6D). As the number of negative samples
 414 is much larger than the number of positive samples, we particularly
 415 recommend investigating the Positive Predictive Value (PPV) of the
 416 predictions. Here, figure 6E shows a moderate PPV that increases
 417 with the cut-off.

418 To perform prediction based on selected patterns using JACUSA2
 419 pipeline, run rule "predict_modification". The patterns can be gen-
 420 erated from a subset of the input data according to the field "inter-
 421 nal_pattern" or predefined patterns indicated in the "external_pattern"
 422 field. The output is a BED file containing the estimated scores and
 423 the corresponding eCDF and PPV plots. The corresponding outputs
 424 are under a new folder called "prediction".

425 `$ srun snakemake --cores all predict_modification`

426 Note that the rules are linked so that the workflow are determined
 427 from top (e.g. predict_modification) to bottom (e.g. sort_bam) and
 428 executed accordingly from bottom to top 4. Therefore, running "pre-
 429 dict_modification" rule leads to excuting all rules in its pipeline.

430 Use Case 2: Comparison of wild-type and IVT samples

431 An alternative way to detect RNA modification is to compare a modi-
 432 fied sample to an *in-vitro* (IVT) synthesized control sample. Therefore,
 433 we benchmark JACUSA2 on a sample set of wild-type HEK293 cell lines
 434 (modified sample) with two replicates (2 and 3) from Pratanwanich et al.
 435 [2021] and a modification-free RNA synthesized sample (control sample).
 436 The analysis steps are similar to case 1. We evaluate the analysis against
 437 miCLIP m6A sites (figure 5).

- 438 1. Identify read error profile: we use JACUSA2 call-2 with the same
 439 parameters as the previously described case. The input BAM files
 440 (HEK293T-WT-rep2.bam, HEK293T-WT-rep3.bam) and (HEK293T-
 441 IVT-rep1.bam, HEK293T-IVT-rep2.bam) are associated to the wild-
 442 type and IVT replicate samples respectively.

443 `$ srun snakemake --cores all jacusa2_call2`

- 444 2. Preprocess JACUSA2 output: we select all sites within the specific 5-
 445 mer (NNANN) and we consider the Y filter that excludes sites within

446 the homo-polymer regions. Then, we extract 5-mer features such that
447 the selected sites are represented by the three scores: mismatch, dele-
448 tion and insertion for the observed site and its two flanking positions
449 from both sides.

450 `$ srun snakemake --cores all get_features`

451 3. Extract m6A modification pattern: using NMF factorization, we ex-
452 tract patterns from 1,905 sites reported as modified in the three miCLIP-
453 based studies. Based on the silhouette and cophenetic correlation in-
454 dices, we could identify an optimal factorization rank of 6 (figure 7A).
455 We determined the predominant factors from matrix W ; accordingly,
456 more than 80% of m6A modification sites can be represented by four
457 patterns (Patterns: 1,2,3,6) (figure 7B). In agreement with case 1, the
458 linear combination of the four patterns confirms the importance of
459 position 3 and the implication of all scores as shown in figure (7C).

460 `$ srun snakemake --cores all get_pattern`

461 4. Predict m6A modifications: we evaluate the prediction ability of the
462 detected patterns on a test set of almost 1,52 million sites where
463 17,021 are miCLIP-m6A modified. We consider the linear combina-
464 tion of the four important patterns (1,2,3,6). Figure 7D shows the
465 eCDF of the inferred scores. The difference between the cumulative
466 distribution of non miCLIP sites and miCLIP sites can be nicely ob-
467 served, while, the PPV plot shows a lower performance as compared
468 to case 1 (figure 7E). The decrease in performance is likely explained
469 by the absence of all modifications and not exclusively m6A in the
470 control condition, which may induce noise to the score estimation by
471 JACUSA2 call-2 .

472 `$ srun snakemake --cores all predict_modification`

CD:to
be con-
firmed

473 NOTES

474 Tips and Tricks

475 ACKNOWLEDGMENTS

476 The authors would like to thank Etienne Boileau, Thiago Britto Borges,
477 Tobias Jakobi for proof-reading and comments. The authors are grateful
478 to Marek Franitza for running the experiments on the 10x platform and to
479 Christian Becker for running ONT sequencing. This work was supported by
480 Informatics for Life funded by the Klaus Tschira Foundation.

REFERENCES

- Minimap2. <https://github.com/lh3/minimap2>. Accessed: 2022-01-19.
- Snakemake. <https://snakemake.readthedocs.io>. Accessed: 2022-01-26.
- Basecalling with guppy. <https://github.com/metagenomics/denbi-nanopore-training/blob/master/docs/basecalling/basecalling.rst>, 2019. Accessed: 2022-01-19.
- Jacusa2 manual. <https://github.com/dieterich-lab/JACUSA2>, 2021. Accessed: 2022-01-15.
- Samir Adhikari, Wen Xiao, Yong-Liang Zhao, and Yun-Gui Yang. m(6)a: Signaling for mrna splicing. *RNA biology*, 13:756–759, September 2016. ISSN 1555-8584. doi: 10.1080/15476286.2016.1201628.
- Ina Anreiter, Quoseena Mir, Jared T. Simpson, Sarath C. Janga, and Matthias Soller. New twists in detecting mrna modification dynamics. *Trends in biotechnology*, 39:72–89, January 2021. ISSN 1879-3096. doi: 10.1016/j.tibtech.2020.06.002.
- Konstantinos Boulas, Diana Toczyłowska-Socha, Ben R Hawley, Noa Liberman, Ken Takashima, Sara Zaccara, Théo Guez, Jean-Jacques Vasseur, Françoise Debart, L Aravind, et al. Identification of the m6am methyltransferase pcif1 reveals the location and functions of m6am in the transcriptome. *Molecular cell*, 75(3):631–643, 2019.
- Jean-Philippe Brunet, Pablo Tamayo, Todd R Golub, and Jill P Mesirov. Metagenes and molecular pattern discovery using matrix factorization. *Proceedings of the national academy of sciences*, 101(12):4164–4169, 2004.
- Dan Dominissini, Sharon Moshitch-Moshkovitz, Schraga Schwartz, Mali Salmon-Divon, Lior Ungar, Sivan Osenberg, Karen Cesarkas, Jasmine Jacob-Hirsch, Ninette Amariglio, Martin Kupiec, Rotem Sorek, and Gideon Rechavi. Topology of the human and mouse m6a rna methylomes revealed by m6a-seq. *Nature*, 485:201–206, April 2012. ISSN 1476-4687. doi: 10.1038/nature11112.
- Attila Frigyesi and Mattias Höglund. Non-negative matrix factorization for the analysis of complex gene expression data: identification of clinically relevant tumor subtypes. *Cancer informatics*, 6:CIN–S606, 2008.
- David Garcias Morales and José L. Reyes. A birds’-eye view of the activity and specificity of the mrna m, javax.xml.bind.jaxbelement@6d66739e, a methyltransferase complex. *Wiley interdisciplinary reviews. RNA*, 12: e1618, January 2021. ISSN 1757-7012. doi: 10.1002/wrna.1618.

517 Guifang Jia, Ye Fu, Xu Zhao, Qing Dai, Guanqun Zheng, Ying Yang,
518 Chengqi Yi, Tomas Lindahl, Tao Pan, Yun-Gui Yang, and Chuan He.
519 N6-methyladenosine in nuclear rna is a major substrate of the obesity-
520 associated fto. *Nature chemical biology*, 7:885–887, October 2011. ISSN
521 1552-4469. doi: 10.1038/nchembio.687.

522 Shengdong Ke, Endalkachew A. Alemu, Claudia Mertens, Emily Conn Gant-
523 man, John J. Fak, Aldo Mele, Bhagwattie Haripal, Ilana Zucker-Scharff,
524 Michael J. Moore, Christopher Y. Park, Cathrine Broberg Vågbo, Anna
525 Kussnierzcyk, Arne Klungland, James E. Darnell, and Robert B. Darnell.
526 A majority of m6a residues are in the last exons, allowing the potential
527 for 3’ utr regulation. *Genes & development*, 29:2037–2053, October 2015.
528 ISSN 1549-5477. doi: 10.1101/gad.269415.115.

529 Casslynn WQ Koh, Yeek Teck Goh, and WS Sho Goh. Atlas of quantitative
530 single-base-resolution n 6-methyl-adenine methylomes. *Nature communi-
531 cations*, 10(1):1–15, 2019.

532 Nadine Körtel, Cornelia Rücklé, You Zhou, Anke Busch, Peter Hoch-Kraft,
533 Reymond FX Sutandy, Jacob Haase, Mihika Pradhan, Michael Musheev,
534 Dirk Ostareck, et al. Deep and accurate detection of m6a rna modifications
535 using miclip2 and m6aboost machine learning. *bioRxiv*, pages 2020–12,
536 2021.

537 Johannes Köster and Sven Rahmann. Snakemake—a scalable bioinformatics
538 workflow engine. *Bioinformatics*, 28(19):2520–2522, 2012.

539 Daniel D Lee and H Sebastian Seung. Learning the parts of objects by
540 non-negative matrix factorization. *Nature*, 401(6755):788–791, 1999.

541 Kate D. Meyer, Yogesh Saletore, Paul Zumbo, Olivier Elemento, Christo-
542 pher E. Mason, and Samie R. Jaffrey. Comprehensive analysis of mrna
543 methylation reveals enrichment in 3’ utrs and near stop codons. *Cell*, 149:
544 1635–1646, June 2012. ISSN 1097-4172. doi: 10.1016/j.cell.2012.05.003.

545 Michael Piechotta, Qi Wang, Janine Altmüller, and Christoph Dieterich.
546 Rna modification mapping with jacusa2. *bioRxiv*, 2021.

547 Ploy N Pratanwanich, Fei Yao, Ying Chen, Casslynn WQ Koh, Yuk Kei
548 Wan, Christopher Hendra, Polly Poon, Yeek Teck Goh, Phoebe ML Yap,
549 Jing Yuan Chooi, et al. Identification of differential rna modifications
550 from nanopore direct rna sequencing with xpore. *Nature Biotechnology*,
551 39(11):1394–1402, 2021.

552 Jean-Yves Roignant and Matthias Soller. m,
553 javax.xml.bind.jaxbelement@8cec19d, a in mrna: An ancient mech-
554 anism for fine-tuning gene expression. *Trends in genetics : TIG*, 33:
555 380–390, June 2017. ISSN 0168-9525. doi: 10.1016/j.tig.2017.04.003.

556 Ian A. Roundtree, Molly E. Evans, Tao Pan, and Chuan He. Dynamic rna
557 modifications in gene expression regulation. *Cell*, 169:1187–1200, June
558 2017. ISSN 1097-4172. doi: 10.1016/j.cell.2017.05.045.

559 Peter J Rousseeuw. Silhouettes: a graphical aid to the interpretation and
560 validation of cluster analysis. *Journal of computational and applied math-*
561 *ematics*, 20:53–65, 1987.

562 Hailing Shi, Jiangbo Wei, and Chuan He. Where, when, and how:
563 Context-dependent functions of rna methylation writers, readers, and
564 erasers. *Molecular cell*, 74:640–650, May 2019. ISSN 1097-4164. doi:
565 10.1016/j.molcel.2019.04.025.

566 Sara Zaccara, Ryan J. Ries, and Samie R. Jaffrey. Reading, writing and
567 erasing mrna methylation. *Nature reviews. Molecular cell biology*, 20:608–
568 624, October 2019. ISSN 1471-0080. doi: 10.1038/s41580-019-0168-5.

569 Zhang Zhang, Tao Chen, Hong-Xuan Chen, Ying-Yuan Xie, Li-Qian Chen,
570 Yu-Li Zhao, Biao-Di Liu, Lingmei Jin, Wutong Zhang, Chang Liu,
571 et al. Systematic calibration of epitranscriptomic maps using a synthetic
572 modification-free rna library. *Nature Methods*, 18(10):1213–1222, 2021.

573 Guanqun Zheng, John Arne Dahl, Yamei Niu, Peter Fedorcsak, Chun-Min
574 Huang, Charles J. Li, Cathrine B. Vågbo, Yue Shi, Wen-Ling Wang, Shu-
575 Hui Song, Zhike Lu, Ralph P. G. Bosmans, Qing Dai, Ya-Juan Hao, Xin
576 Yang, Wen-Ming Zhao, Wei-Min Tong, Xiu-Jie Wang, Florian Bogdan,
577 Kari Furu, Ye Fu, Guifang Jia, Xu Zhao, Jun Liu, Hans E. Krokan, Arne
578 Klungland, Yun-Gui Yang, and Chuan He. Alkbh5 is a mammalian rna
579 demethylase that impacts rna metabolism and mouse fertility. *Molecular*
580 *cell*, 49:18–29, January 2013. ISSN 1097-4164. doi: 10.1016/j.molcel.2012.
581 10.015.

FIGURE CAPTIONS

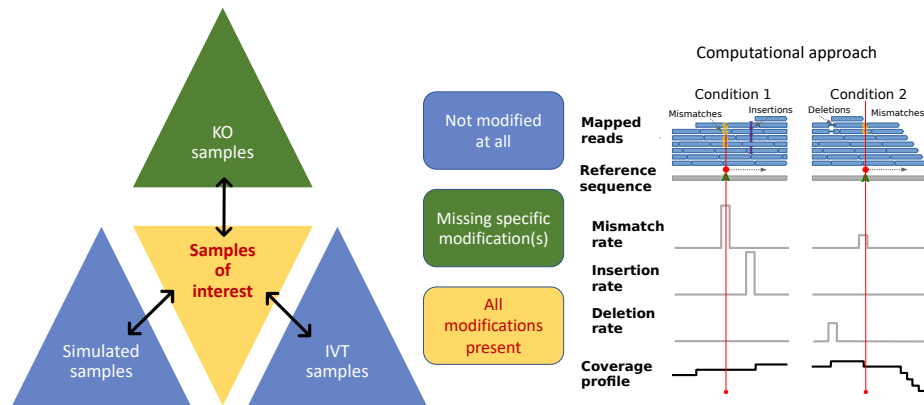


Figure 1: **General outline of RNA modification detection by JACUSA2.** A key feature of our approach is that multiple replicates can be compared as shown on the left. Samples of interests where all modifications are present could be compared with either KO samples where the modification of interest is missing or IVT/simulated samples where all modifications are absent. Read stacks (in blue) are compared head-to-head as shown on the right.

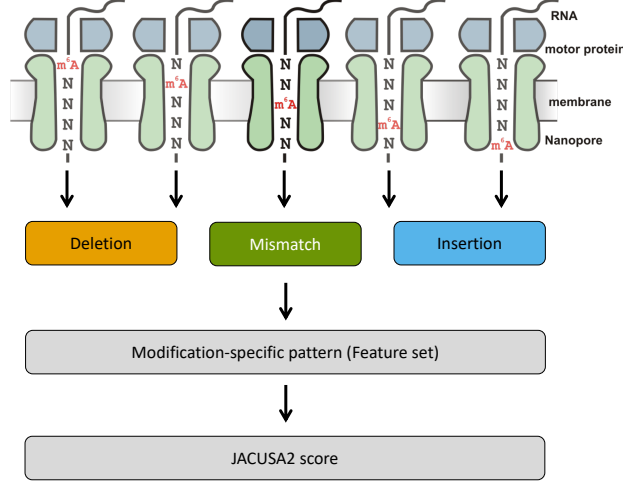


Figure 2: **Motivation of 5-mer context for RNA modification mapping.** The nanopore covers 5 consecutive RNA residues. That is why we consider a 5-mer context and derive 3 principal features for every position within a given 5-mer (15 features in total, with a central A residue in this example). We evaluate each feature set by previously learned patterns and compute a final score for modification site detection.

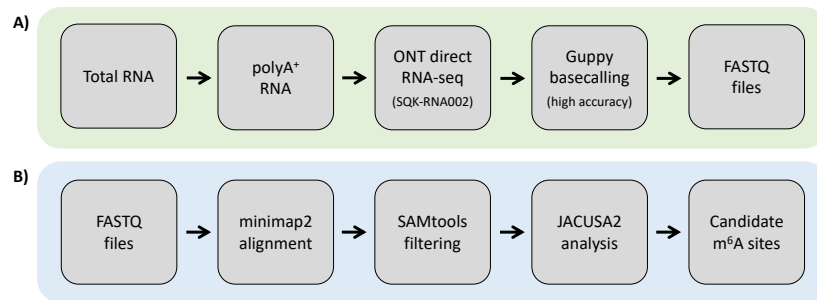


Figure 3: **Experimental and computational workflow.** tbd

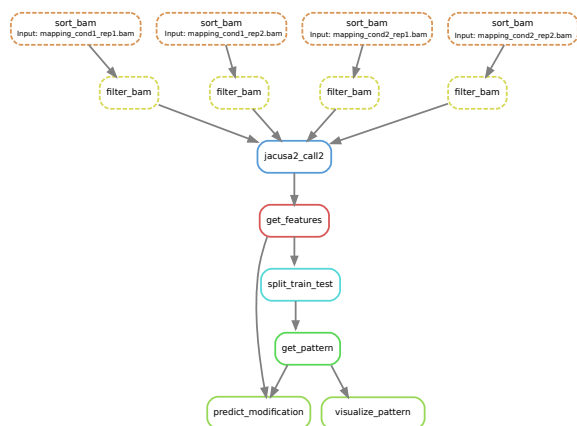


Figure 4: **Computational workflow.** Snakemake workflow for RNA modification detection based on JACUSA2 variant calling.

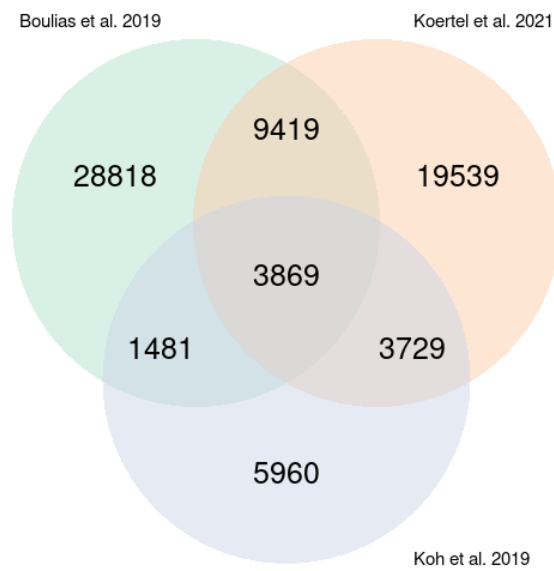


Figure 5: m6A sites reported in the three miCLIP-based studies: Boulias et al. [2019], Koh et al. [2019] and Körtel et al. [2021].

Software	Version	Description
Minimap2	https://github.com/lh3/minimap2 v2.22 or later	https://lh3.github.io/minimap2/
samtools	https://github.com/samtools/samtools v1.12 or later	http://samtools.github.io/
JAVA	openjdk 11.0.12 2021-07-20 - JAVA 11 or later	OpenJDK Runtime Environment
R	https://www.r-project.org/ version 3.5.1 or later	The R Project for Statistical Computing
PERL	https://www.perl.org/ version 5.28.1 or later	Perl is a highly capable, feature-rich programming language
BASH, sed, awk	should be part of your Linux distribution	Misc.
bedtools	https://github.com/arq5x/bedtools2 version 2.29.2 or later	Perl is a highly capable, feature-rich programming language
NanoSim	https://github.com/bcgsc/NanoSim version 3.0.2 or later (optional)	NanoSim is a fast and scalable read simulator that captures the technology-specific features of ONT data

Table 1: **Software dependencies** blubba

583 TABLE CAPTIONS

584 TABLES

R Pack- ages	Version	Description
ggplot2	https://cran.r-project.org/web/packages/ggplot2/index.html - ggplot2_3.3.0 or later	ggplot2 is a system for declaratively creating graphics, based on The Grammar of Graphics.
NMF	https://cran.r-project.org/web/packages/NMF/index.html - NMF_0.22.0 or later	Provides a framework to perform Non-negative Matrix Factorization (NMF).

Table 2: **R Package dependencies** blubba

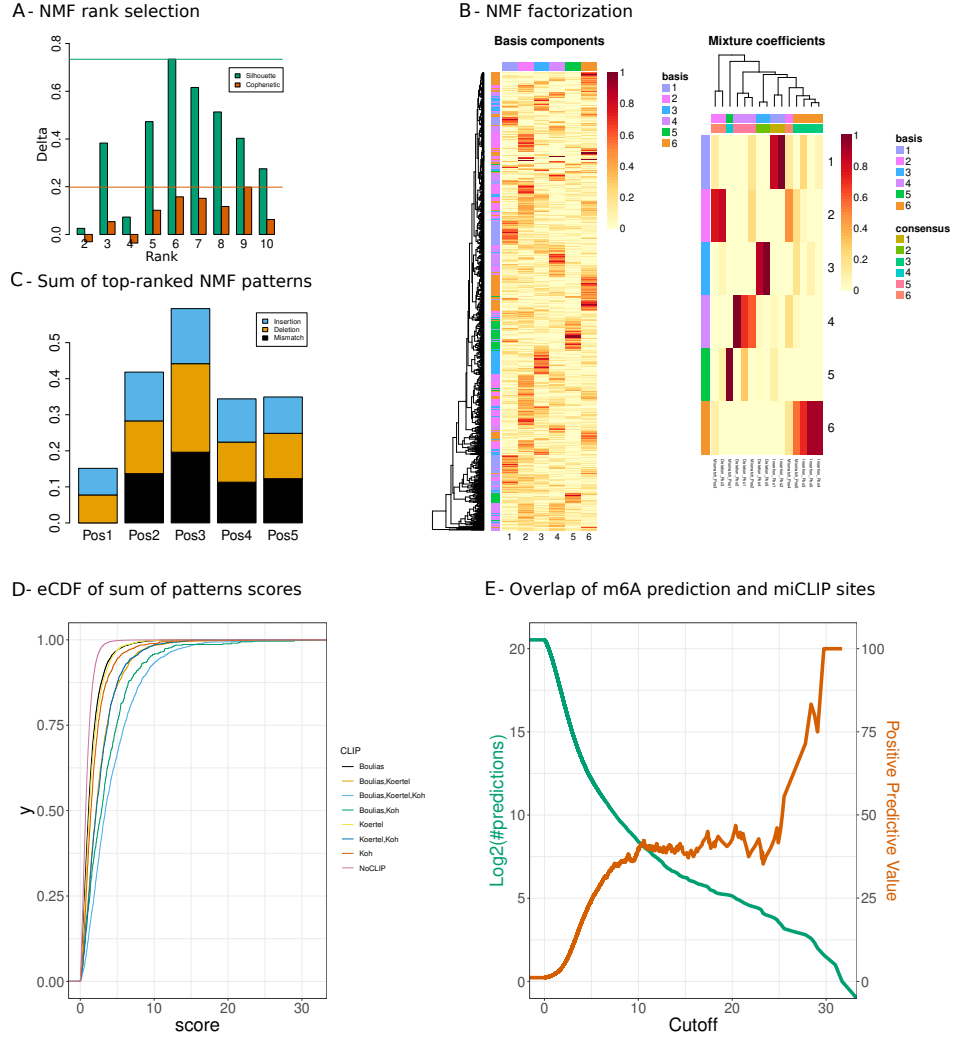


Figure 6: Case 1. WT versus KO. A: NMF rank selection. Barplots representing the difference of cophenetic correlation and silhouette indices between the NMF factorization of the original and the randomized data. Ranks with the largest value for both indices are determined, then the smallest rank is selected for the NMF decomposition. **B:** NMF result represented by the basis matrix W and the coefficient matrix H . The matrix H induces the RNA modification pattern. **C:** Barplots representing the linear combination of the top 5 patterns (y-axis) by the number of position in the specific 5-mer context (x-axis) and the score type: mismatch, deletion and insertion (resp. black, orange and blue). The 5 patterns (coefficient vectors: 1,2,3,4,6) are selected according to the predominant columns in matrix W . **D:** Score distribution inferred from the combined patterns, stratified by the different categories of miCLIP validated sites and non miCLIP sites. **E:** Number of predicted m6A sites (green) and Positive Predictive Value (PPV) of predicted m6A sites that overlap with miCLIP sites (orange).

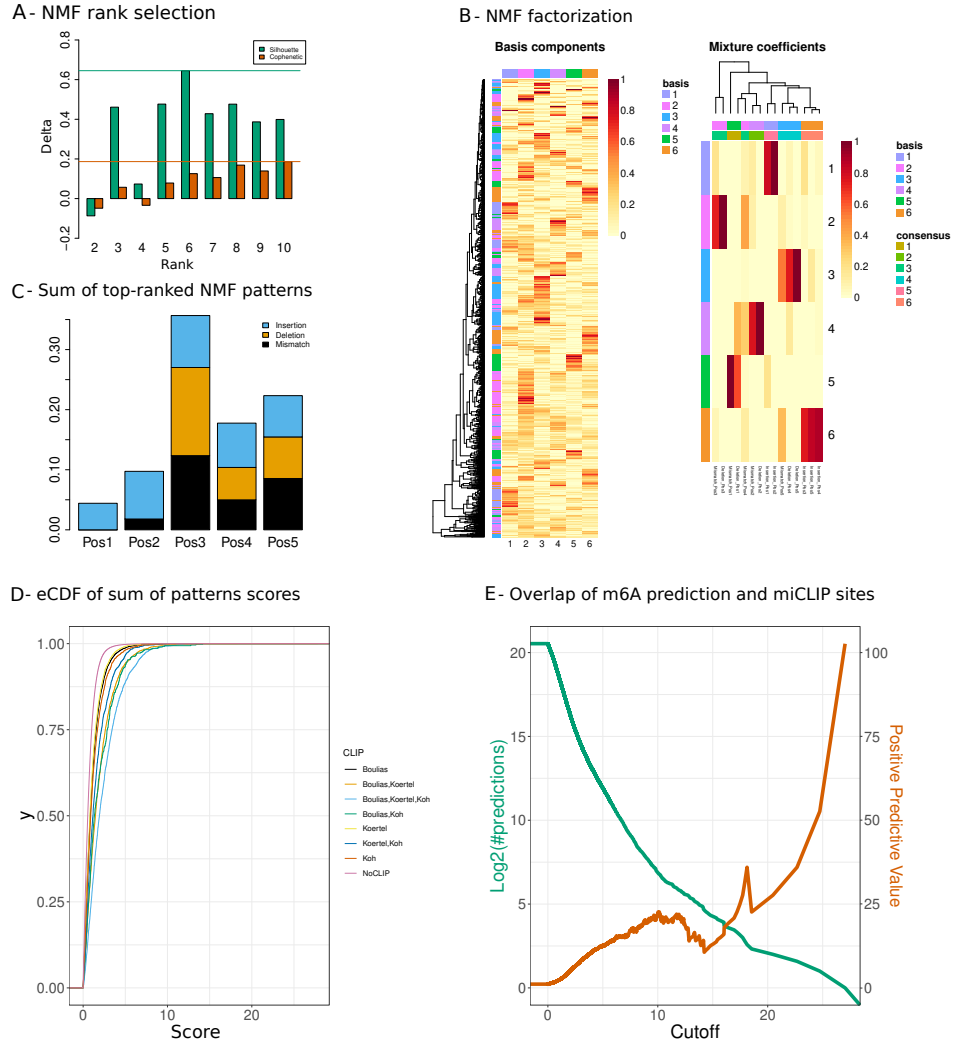


Figure 7: Case 2. WT versus IVT. A: NMF rank selection. Barplots representing the difference of cophenetic correlation and silhouette indices between the NMF factorization of the original and the randomized data. Ranks with the largest value for both indices are determined, then the smallest rank is selected for the NMF decomposition. **B:** NMF result represented by the basis matrix W and the coefficient matrix H . The matrix H induces the RNA modification pattern. **C:** Barplots representing the linear combination of the top 4 patterns (y-axis) by the number of position in the specific 5-mer context (x-axis) and the score type: mismatch, deletion and insertion (resp. black, orange and blue). The 4 patterns (coefficient vectors: 1,2,3,6) are selected according to the predominant columns in matrix W . **D:** Score distribution inferred from the combined patterns, stratified by the different categories of miCLIP validated sites and non miCLIP sites. **E:** Number of predicted m6A sites (green) and Positive Predictive Value (PPV) of predicted m6A sites that overlap with miCLIP sites (orange).